Quantifying imperfect camera-trap detection probabilities: implications for density modelling

T. McIntyre [A B E] , T. L. Majelantle [B] , D. J. Slip [C D] and R. G. Harcourt [D]

[A] Department of Life and Consumer Sciences, College of Agriculture and Environmental Sciences, University of South Africa, Private Bag X6, Florida, 1710, South Africa.

[B] Mammal Research Institute, Department of Zoology and Entomology, University of Pretoria, Private Bag X20, Hatfield, 0028, South Africa.

[C] Taronga Conservation Society Australia, Bradley's Head Road, Mosman, NSW 2088, Australia.

[D] Marine Predator Research Group, Department of Biological Sciences, Macquarie University, North Ryde, NSW 2113, Australia.

[E] Corresponding author. Email: trevmcnt@gmail.com

Abstract

Context: Data obtained from camera traps are increasingly used to inform various population-level models. Although acknowledged, imperfect detection probabilities within camera-trap detection zones are rarely taken into account when modelling animal densities.

Aims: We aimed to identify parameters influencing camera-trap detection probabilities, and quantify their relative impacts, as well as explore the downstream implications of imperfect detection probabilities on population-density modelling.

Methods: We modelled the relationships between the detection probabilities of a standard camera-trap model ($n = 35$) on a remotely operated animal-shaped soft toy and a series of parameters likely to influence it. These included the distance of animals from camera traps, animal speed, camera-trap deployment height, ambient temperature (as a proxy for background surface temperatures) and animal surface temperature. We then used this detection-probability model to quantify the likely influence of imperfect detection rates on subsequent population-level models, being, in this case, estimates from random encounter density models on a known density simulation.

Key results: Detection probabilities mostly varied predictably in relation to measured parameters, and decreased with an increasing distance from the camera traps and speeds of movement, as well as heights of camera-trap deployments. Increased differences between ambient temperature and animal surface temperature were associated with increased detection probabilities. Importantly, our results showed substantial inter-camera (of the same model) variability in detection probabilities. Resulting model outputs suggested consistent and systematic underestimation of true population densities when not taking imperfect detection probabilities into account.

Conclusions: Imperfect, and individually variable, detection probabilities inside the detection zones of camera traps can compromise resulting population-density estimates.

Implications: We propose a simple calibration approach for individual camera traps before field deployment and encourage researchers to actively estimate individual camera-trap detection performance for inclusion in subsequent modelling approaches.

Additional keywords: detectability, mark–recapture, performance, random encounter model.

Introduction

Camera traps are now an essential tool in ecology and conservation, and are widely used in ecological studies designed to assess animal diversity, species occupancy, densities and even animal behaviours (see reviews by Trolliet *et al.* 2014; Burton *et al.* 2015; Marvin *et al.* 2016; Caravaggi 2017). They are robust, economical and relatively non-intrusive, and can produce otherwise unobtainable datasets so large that deep learning approaches are needed to aid automated image identification (Norouzzadeh *et al.* 2018; Tabak *et al.* 2018). Accordingly, there has been huge growth in the deployment of camera traps in terrestrial field studies, but accompanying this there has been increased scrutiny of study designs and their inherent assumptions (Foster *et al.* 2012; Hamel *et al.* 2013; Hofmeester *et al.* 2019). Inappropriate design may result in poor detectability and, so, camera-trap sampling designs must be rigorously tested to optimise detection of the target species (Stokeld *et al.* 2015; Apps and McNutt 2018). Arising from this need for improved rigour is the need to account for imperfect detection probabilities of study organisms. These detection probabilities can occur at two levels, namely (1) where individuals or species present are not detected because of them not entering the small camera-trap detection zone, and (2) where individuals do pass through the camera-trap detection zones, but are not detected (Burton *et al.* 2015). Some modelling approaches, particularly occupancy models, explicitly model the overall detection probabilities of study animals (i.e. the likelihood of detecting a species if present in the study area; O'Connell and Bailey 2011; Lewis *et al.* 2015). However, many study designs implicitly assume that the probability of detecting study animals *within the detection zones of camera traps* is perfect (i.e. that any study animal passing within the detection zone of an individual camera trap will be detected), or at least nearly so (e.g. Neilson Avgar Burton Broadley and Boutin 2018). Whereas this assumption is more often than not, not met (Rowcliffe *et al.* 2011; Burton *et al.* 2015; Jacobs and Ausband 2018), it has largely been dealt with only conceptually (Hofmeester *et al.* 2019), and we are not aware of any field studies that have explicitly taken this into account when using camera-trap data for estimating population densities.

Variables known to influence detection probabilities of animals in camera-trap data include animal size (Rowcliffe *et al.* 2011; Anile and Devillard 2016) and the distances of study animals from camera traps within their detection zones (Randler and Kalb 2018). Moreover, the behaviour of animals when they detect camera traps is likely to influence repeat detections (Meek *et al.* 2014, 2016*a*). High ambient temperatures are generally considered to have a negative influence on detections, as lower background surface temperatures tend to create a bigger infrared-light contrast with animals (typically endothermic) characterised by higher surface temperatures (Swann *et al.* 2004). Although not a measure of camera-trap performance, warmer ambient conditions may also lead to increased activity levels of study organisms, thereby leading to increased detection numbers (Randler and Kalb 2018). Another variable likely to influence detection probabilities in camera-trap data is the variability in probabilities associated with differences in camera-trap models (Meek *et al.* 2015; Driessen

et al. 2017). Last, higher average movement speeds of study animals may generate potentially lower detection probabilities (Rowcliffe *et al.* 2011).

Here, we investigated detection probabilities associated with standard, mid-range camera traps, and aimed to quantify the influences of several parameters. These included animal-movement speed, distance from camera traps, camera-trap deployment heights and differences between the surface temperatures of animals and the background surface temperatures. We expected detection probabilities to be influenced by all the above-mentioned parameters and further aimed to explore the likely impacts that imperfect detections have on population-level model outputs. Using random encounter models, we specifically assessed the impacts of modelled detection probabilities on population-level density estimates obtained for known population densities.

Materials and methods

Camera-trap detectability trials

We used 35 Primos ProofCam 3 camera-traps (Primos Hunting, Flora, MS, USA) set on a homogenous environment (LC de Villiers sports field, University of Pretoria) to assess variation in camera-trap detection rates. The trialled camera traps incorporate wide angle, multi-zone Fresnel lenses over the passive infrared sensors and have general specifications typical for mid-range camera-trap models (Table 1).

Table 1. Specifications of the camera-trap model used
Specifications are from the owner's manual, whereas the detection angle and field of view are reported from reviews conducted on 'Trailcampro.com' (https://trailcampro.com, accessed 15 January 2019)

Parameter	Primos Proof Cam 03
Image resolution	Adjustable: max = 12 MP
Flash type	'No glow' infrared
Detection angle	42.8°
Field of view	35°
PIR lens	Multi-zone Fresnel
PIR sensitivity	Auto
Trigger time	0.4 s
Triggering interval	Adjustable: min = 3 s

Camera traps were set at various heights from the ground, such that the centre of each motion sensor was between 20 cm and 80 cm from the ground, and aimed parallel with the ground surface (i.e. no dip or tilt). Camera traps were randomly assigned a setup height of ~20, 40, 60 or 80 cm and placed in position accordingly (the height of the passive infrared sensor (PIR) from the ground was then measured after setup). Camera traps were programmed to take bursts of two images when triggered and to the minimum trigger interval (3 s). We then ran a series of controlled trials (46 trials, resulting in 1988 data points) by using an animal-shaped soft toy (shaped after a Californian sea lion, *Zalophus californianus*) mounted on a radio-controlled vehicle and fitted with a hot water bottle (capacity of 1.5 L, but filled to ~1 L to limit weight on the underlying vehicle) to simulate higher, but heterogenous, animal surface temperatures (Fig. 1). The overall dimensions of this target were 50 cm

(length) × 30 cm (width) × 30 cm (height). Distances of 2, 4, 6, 8 and 10 m in front of the camera traps were marked out with tennis balls. The target was then driven in a straight line parallel to the camera traps and as close as possible to the series of distance markers. Each trial consisted of a single pass of the target at a set distance from the camera traps (between 2 m and 10 m) and travelling at measured speeds and recorded directions (either left to right or right to left). We conducted trials at various times of day, starting at sunrise until midday over two separate days during winter in the Highveld region of South Africa. Daily temperature fluctuations are high during this time of year, when minimum night-time temperatures are regularly below 3°C, rising to maximum temperatures above 20°C during the day. For each of the trials, we measured the ambient temperature, as well as the surface temperature of the hot water bottle mounted on the model by using a Eutech EcoScan Temp 6 thermoprobe (Thermo Fisher Scientific Inc., Franklin, MA, USA) and a Sentry ST642 hybrid infrared thermometer (Sentry Optronics Corp., New Taipei City, Taiwanoration) respectively. Ambient temperature was assumed to represent the background surface temperature, given that background surfaces were too distant (>25 m) to measure conveniently.

Fig. 1. Experimental setup, illustrating the animal model used (*a*); and the array of mounted camera traps (*b*).

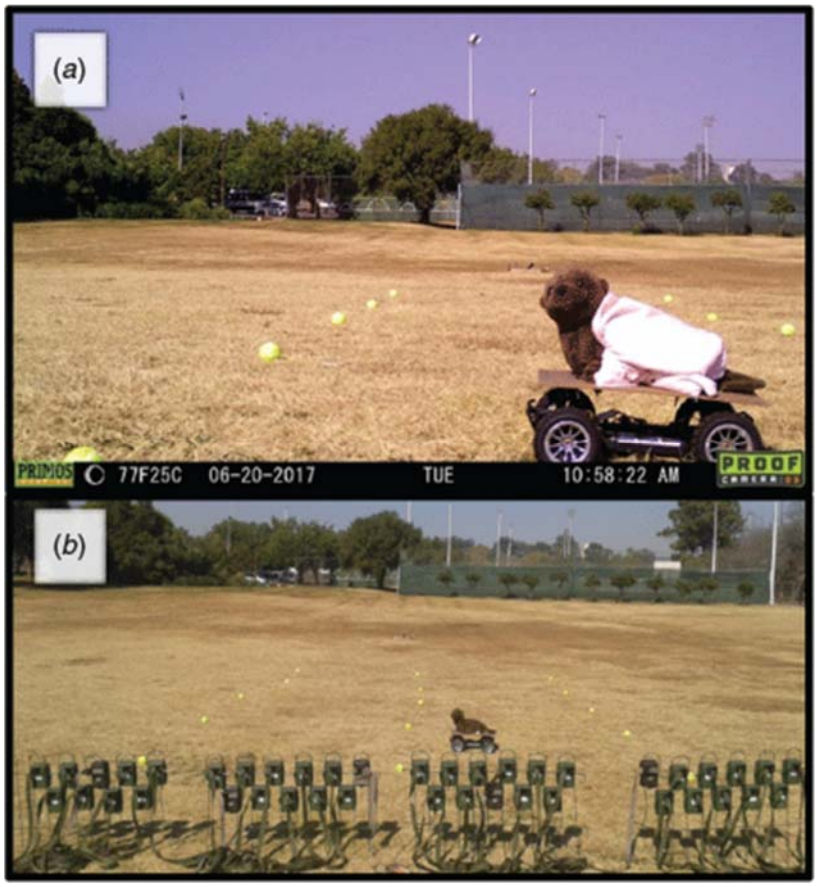

We measured or calculated the following predictor variables for each of the camera-trap trials:

- distance from camera trap (hereafter ‘distance’): 2-m intervals including 2, 4, 6, 8 and 10 m;

- speed of the animal model (hereafter 'speed'): time (in s) to travel set distances for each trial was measured using a hand-held stopwatch, with a recording resolution of two decimals. Speed was subsequently expressed in m s^{-1};
- height of camera-trap deployment (hereafter 'height'): the height of the passive infrared sensor from the ground;
- the difference between the animal model surface temperature and the ambient temperature (hereafter 'ΔTemp'). Given the homogenous nature of the study area (sports field), we assumed the ambient temperature to be a suitable proxy of the background surface temperature, which is important for functioning of the passive infrared sensor (Welbourne *et al.* 2016).

A positive detection was defined as, at least, one image (in the burst of two images when a camera trap was triggered) recording more than a third of the body length of the model animal.

We used a binomial generalised linear mixed-effects model (GLMM), implemented using the 'lme4' package (Bates, Maechler, Bolker and Walker 2015) in the R programming environment (R Core Team 2019) to explore the influences of predictor variables on detection rates, and including individual camera traps as random effects. Our binomial GLMM included 'height', 'distance', 'speed' and 'ΔTemp' as predictor variables, such that

$$\begin{aligned} &\text{Detected} \sim \text{height} + \text{distance} + \text{speed} + \Delta\text{Temp}, \\ &\quad \text{random effect} = \text{CT ID} \end{aligned} \qquad \text{(Model 1)}$$

Model outputs were visualised using the 'sjPlot' interface package (Lüdecke 2018) for generating plots with 'ggplot2' (Wickham 2016).

Simulated detections

We applied the resulting GLMM outputs to predict the likelihood of cameras detecting animals of a size similar to our target passing in front of modelled populations of animals. For this, we generated correlated random-walk movements of 12 animals across a hypothetical environment. Individual tracks were generated in the *adehabitatLT* package (Calenge 2006), given a scaling parameter (*h*) of 1 and a default concentration (*r*) parameter, and allowed to run for a total of 540 000 steps each. Each step was, subsequently, assumed to represent a single movement per second, thereby representing activity periods of 5 h per day over a period of 30 days. Tracks were then projected onto a surface with a pre-placed array of 25 equally spaced locations representing camera traps.

To extract individual positions within the assumed detection ranges of the camera traps, we first retained all track positions that were closer than 11 m from any camera trap (so as to retain positions within a similar distance from camera traps as used in the detection-probability trials), and calculated the radian angle (i.e. bearing where 90° = direct east and −90° = direct west) between the camera trap and track location by using the *geosphere* and *maptools* packages (Lewin-Koh *et al.* 2011; Hijmans Williams and Vennes 2017). We then visually inspected the distributions of all radian angles, identifying the camera trap/track angles with the highest frequency for each camera trap. We used these values as the centre of a defined 50° arc and retained track positions within these arcs. This simulated a more realistic field situation where camera traps are usually placed to face directions that assume some likelihood of study organisms passing (e.g. camera traps are not placed such that they

face directly towards visual barriers, even when deploying camera traps at randomised locations; Cusack *et al.* 2015*a*). We further filtered the track locations to retain only the first track positions in a sequence of locations within the detection range (i.e. within the defined 50° arc and closer than 11 m) that were separated by intervals of 60 s or less.

Next, we used Model 1 to predict the probability of individual locations being detected in two thermal scenarios (ΔTemp = 20°C and ΔTemp = 10°C), on the basis of their distance from the camera traps and speed of movement, and assuming a camera-trap height of 40 cm (chosen as the rounded value from the mean height, 42 cm, of the camera traps used in the detection-probability trials). We then fitted these probabilities to a binomial density distribution for each record, thus identifying each record as either a 'detected presence' or a 'non-detected presence'.

Assessing influence of imperfect detection rates on density estimates

To explore the influence of varying detection rates on subsequent model outputs, we fitted a series of random encounter models to varying densities and three detection scenarios (perfect detection, Δtemp = 25°C detections and Δtemp = 10°C detections) on the basis of the simulated dataset. We fitted these to the full simulated dataset (n = 12 tracks), as well as five subsets of this dataset, sequentially removing two tracks each time up to a minimum of two. Random encounter models are an approach to obtaining population-density estimates for animals that are not individually identifiable (Rowcliffe *et al.* 2008), and have been applied to estimate densities of several mammal populations (e.g. Manzo *et al.* 2012; Cusack *et al.* 2015*b*; Lucas *et al.* 2015; Caravaggi *et al.* 2016; Pfeffer *et al.* 2018). Models were fit using the *remBoot* package (Caravaggi 2017) and assuming daily travel distances of 0.17 km (calculated as average total straight-line distance travelled per day by all simulated tracks) and a 100% functionality of simulated camera traps for a sampling period of 30 days (therefore equalling 18 000 h). We used a bootstrapping approach (1000 iterations with replacement) to estimate standard deviations of density estimates. All statistical analyses were performed in the R programming environment (R Core Team 2019).

Results

Detection probabilities

Animal model travel speeds averaged 1.04 ± 0.58 m s^{-1} (range: 0.08–3.66 m s^{-1}) during the detection-probability trials. Ambient temperatures averaged 19.3 ± 7°C (range: 0.3–24.8°C) and animal-model surface temperatures averaged 31.2 ± 4.8°C (range: 16–38°C). This resulted in ΔTemp values averaging 11.3 ± 3.3°C (range: 5.42–22.9°C). Overall detection success rate in our trials was 58.2%.

The GLMM outputs illustrated significant relationships between all predictors (distance, speed, height and ΔTemp) and detection success rates (Table 2, Fig. 2). Speed had a strong influence on detection rate, with increasing speeds associated with a decreased detection success. Similarly, increased distance from camera traps was associated with decreased detection rates. Detection rates were positively related to ΔTemp values, increasing with greater differences between the model surface temperature and the ambient temperature. Estimated between-camera trap deviation was 1.1 (Table 2), suggesting (relative to other

effect sizes, which ranged between −0.96 and 0.13) that there was substantial variation in detection probabilities among individual camera traps (Fig. 3). Predicted detection probabilities for individual camera traps in relation to fixed effects are presented as Figs S1–S3, available as Supplementary material to this paper.

Table 2. Coefficient estimates and Wald χ^2 test outputs from generalised linear mixed-effects model (GLMM) assessing parameter influences on camera-trap detection success rates

Standard errors are reported for all parameters, except for the random effect where the standard deviation is reported

Parameter	Estimate	s.e.	CI (2.5%)	CI (97.5%)	χ^2	
Intercept	2.52	0.45	1.64	3.4		
Random effect (CT ID)	1.11	1.05(s.d.)	0.81	1.4		
Distance	−0.34	0.13	−0.39	−0.3	238.08	<
Speed	−0.96	0.13	−1.22	−0.71	53.84	<
Height	−0.02	<0.01	−0.03	−0.01	10.66	<
ΔTemp	0.13	0.03	0.08	0.18	23.55	<

Fig. 2. Predicted detection probabilities (model 1) illustrating decreased detection probabilities at higher travel speeds and increased distances from camera traps (by colour) for three thermal scenarios (Δtemp = 8°C, 11°C and 14°C).

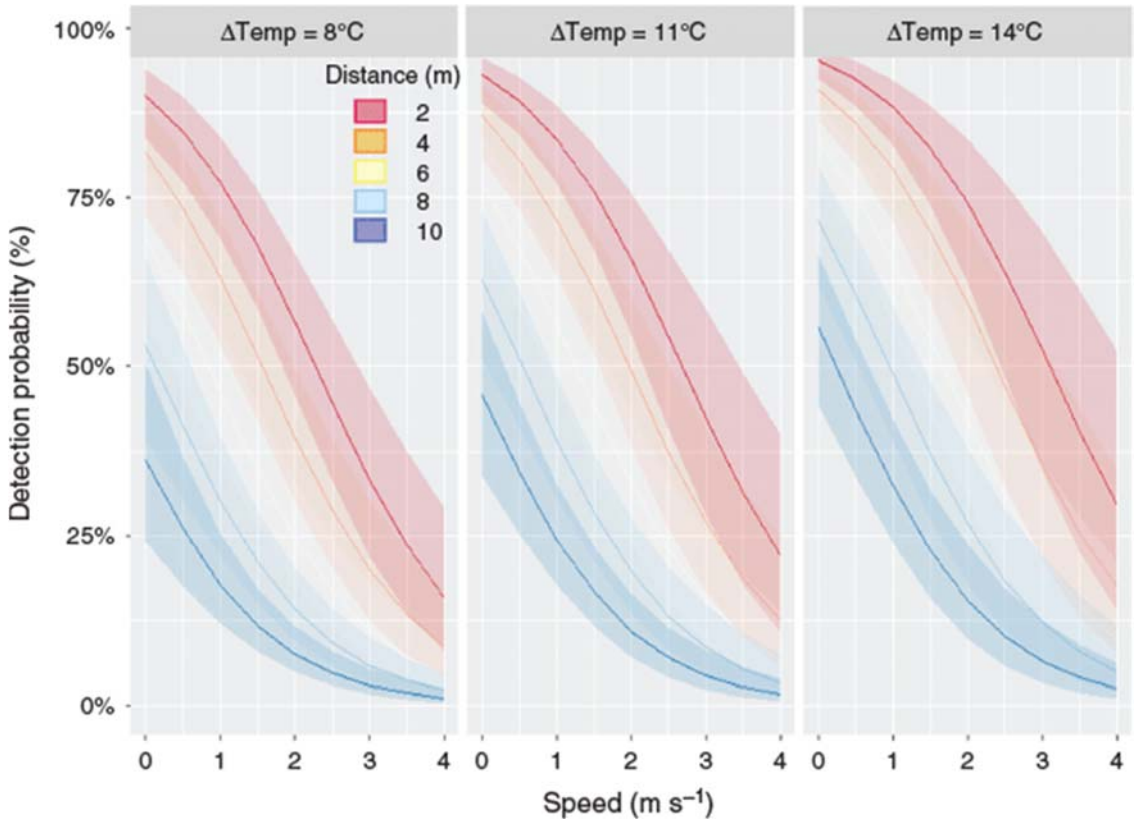

Fig. 3. Random effects plot generated from model 1 (GLMM) illustrating the heterogeneity in performance between individual camera traps.

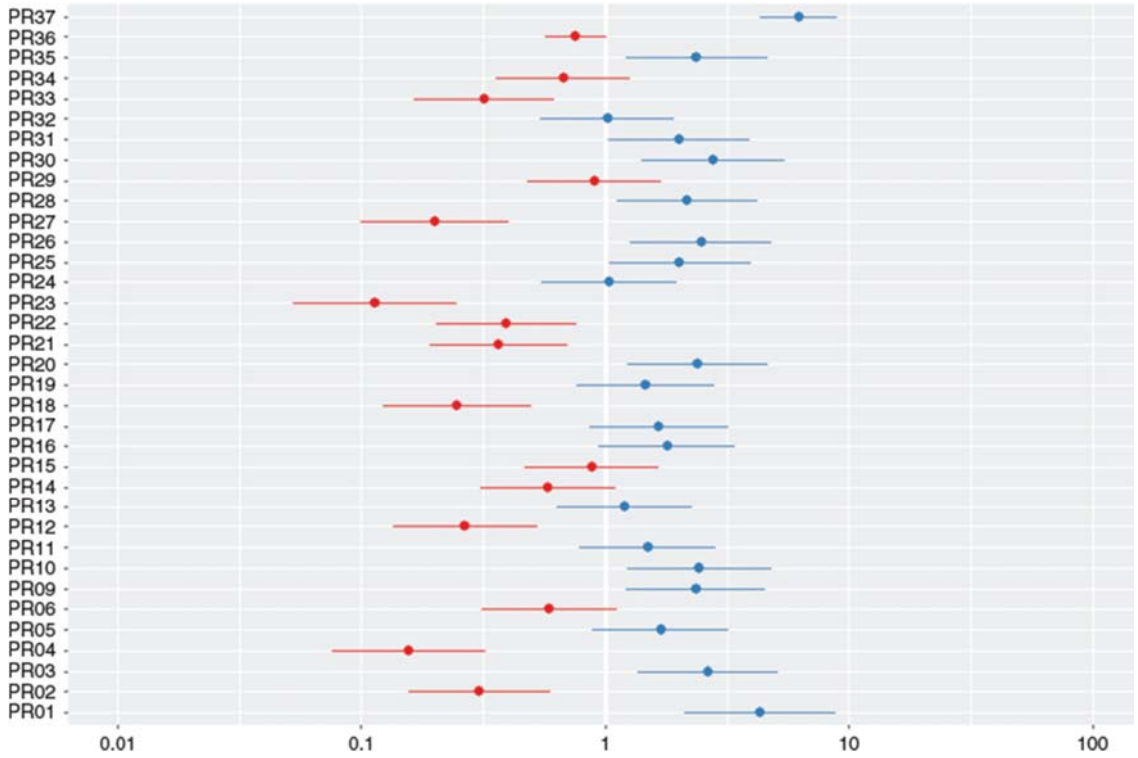

Simulation

Simulated animal trajectories are presented in Fig. 4. Random encounter model density estimates (±s.d.) under a perfect detection scenario included the true density for three of the simulated densities (Fig. 5), but slightly overestimated the density for scenarios of 12 (estimated as 13.2 ± 0.5), four (estimated as 4.8 ± 0.2) and two (estimated as 2.3 ± 01) animals respectively. Estimated densities under the two alternative modelled scenarios (ΔTemp = 25°C and ΔTemp = 10°C) were mostly lower than the true densities (Fig. 5), except the estimated density for a true density of four animals in the ΔTemp = 25°C scenario when the predicted density of 4.1 ± 0.2 included the true density. On average, density estimates for the ΔTemp = 25°C scenario were 14.4% lower than was the true simulated density, whereas density estimates for the ΔTemp = 10°C scenario were 52.6% lower than were the true simulated densities (Fig. 5).

Fig. 4. Simulated animal trajectories for six animal-density estimate scenarios. Animal trajectories (indicated in grey) were obtained using a correlated random-walk simulation. Each individual track consists of 540 000 steps, generated using a scaling parameter (*h*) of assumed here to represent a single movement per second. Triangles illustrate the positions, but not the detection zones, of equally spaced (250 m apart) camera traps in the simulated environment.

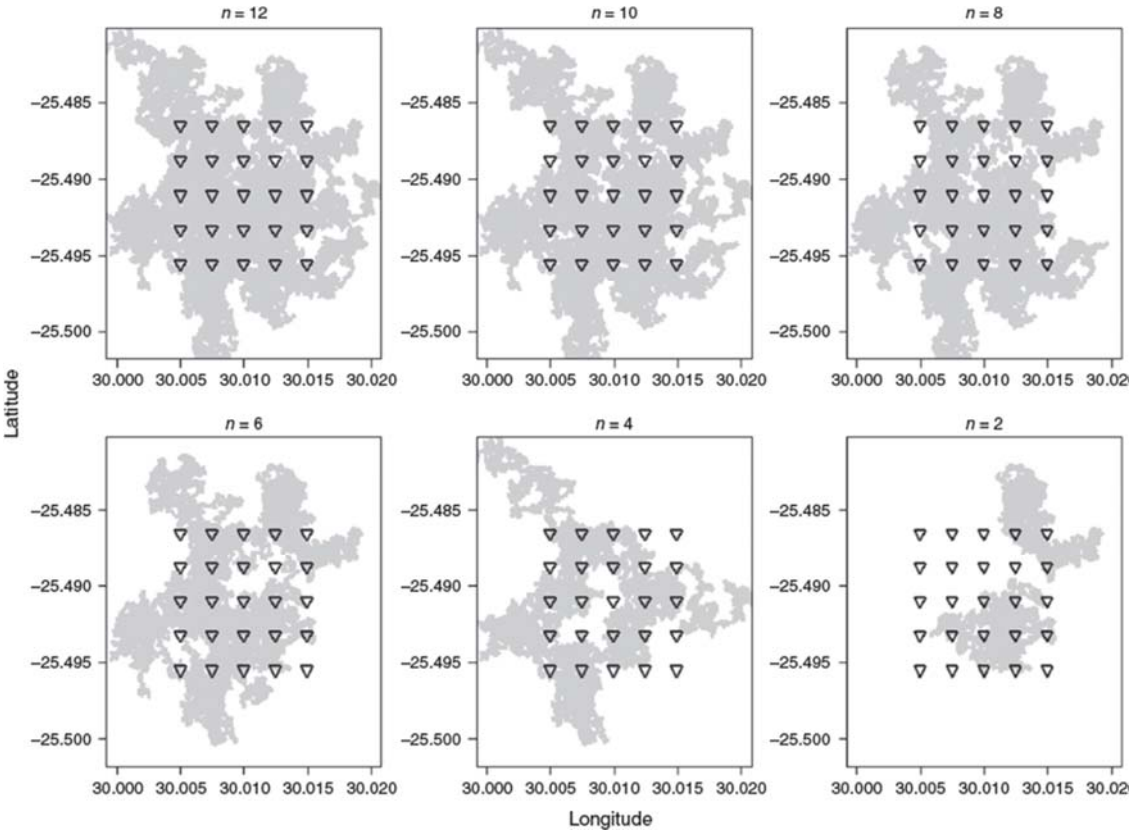

Fig. 5. Random encounter model density estimates under three scenarios for each of the six true densities represented in Fig. 4. Initial detections were defined as track presences (spaced more than 60 s apart) within a defined detection zone (see Materials and methods). Predicted detections were generated using *Model 1* and fitting a binomial model to resulting detection probabilities under the two thermal scenarios (ΔTemp = 25°C and ΔTemp = 10°C). ΔTemp = the difference between ambient temperature and the modelled animal surface temperatures (surface temperature – ambient temperature).

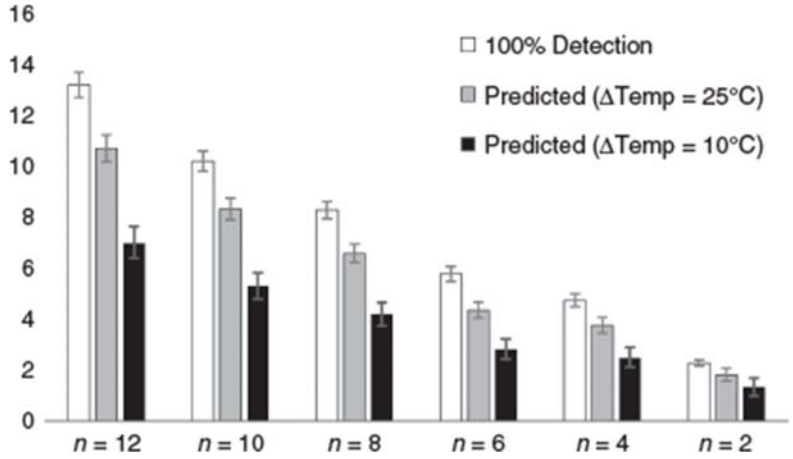

Discussion

Detection probabilities for our model sea lion within the overall detection ranges of the camera traps were smaller than one, as has been found in other studies (Rowcliffe *et al.* 2011; Hamel *et al.* 2013; Burton *et al.* 2015; Jacobs and Ausband 2018). Detection probabilities are sensitive to camera-trap deployment height and negatively associated with distance from the camera traps, as well as speed of animal movement and differences between the surface temperature of animals and background surface temperatures. Although many of these relationships are not unexpected and have been reported on and discussed by others (Hamel *et al.* 2013; Randler and Kalb 2018; Hofmeester *et al.* 2019), some are less well understood. For example, the influence of camera-trap deployment height on detections is inconclusive in the literature, with some studies reporting negative associations (Meek *et al.* 2016*b*), and more recent studies reporting no influence on detections (Jacobs and Ausband 2018). Although we did not assess detection from the heights (up to 3 m) used in other studies (our camera traps were deployed at maximum heights of 80 cm), our results did suggest a general decrease in detection rates with an increased deployment height. This may be compensated for if camera traps are carefully tilted with an appropriate angle of coverage, although such tilting results in further restriction to detectible heights and angles (Apps and McNutt 2018).

The need to account for imperfect detection probabilities when using camera-trap data for subsequent population-level modelling exercises is an important finding of the present study. We specifically used a random encounter model framework to establish whether imperfect detection probabilities (within the detection ranges of camera traps) are likely to result in substantial influences on outputs obtained from modelling exercises that assume perfect or near-perfect detection probabilities within the detection ranges (e.g. distance sampling approaches that assume certain detection at close distance; Howe *et al.* 2017). Although occupancy models and mark–recapture modelling approaches do account for site detection probabilities that are smaller than one (i.e. an organism being present on a site, but not detected, MacKenzie *et al.* 2002), it is useful to understand the scope of bias specifically associated with imperfect detection probabilities inside of camera-trap detection ranges. The random encounter models under a perfect detection scenario did not capture the true densities for three of the modelled densities (two, four and 12 animals). However, the errors of these estimates ranged between 0.2 animals per km^2 (for a true density of 2 animals per km^2) and 0.7 animals per km^2 (for a true density of 12 animals per km^2) from the true values, and we, therefore, consider the estimates rendered to be sufficiently accurate for most field applications. Importantly, when computing random encounter model estimates based on likely detections for two different temperature scenarios, we demonstrated systematic under-estimation of true densities because of imperfect detection probabilities within the detection ranges of camera traps.

Differences in performance among different models of camera trap are well known (e.g. Driessen *et al.* 2017; Apps and McNutt 2018). Importantly, our results showed marked differences in performance also among individual camera traps of the same model and specifications. This supports the outcomes of Hughson *et al.* (2010), who suggested there may be such performance differences on the basis of a comparison of animals captured visiting a water source monitored by up to 10 camera traps consisting of six different models. Therefore, accounting for performance variability of the camera traps themselves could have a major influence on the precision of population and other estimates. Our study design did not include moving individual camera traps among mounting locations in the array that we used, and it is, therefore, possible that some correlation exists between the individual mounting

locations and the performance of individual camera traps. However, we consider the environment in which the trials were conducted to be sufficiently homogenous and, therefore, unlikely to be influenced by substantial differences in microsite characteristics (such as e.g. influences of camera trap-specific temperatures) for this to have played an important role in explaining the inter-camera-trap variation in performance. Performance differences among camera trap models can be substantial (Driessen *et al.* 2017) and it is possible that some camera-trap models are sufficiently similar in overall performance so that individual-level camera-trap performance does not influence resulting outputs. However, our results suggest that best practice in camera-trap study design should incorporate calibrating individual camera traps before field deployment to enable correction for differences in detection performance among traps *post hoc*. At the very least, an assessment of individual variability in detection would enable subsequent model building to include a realistic estimate of camera trap-performance variability as a covariate (Fig. 6).

Fig. 6. Best-practice guidelines for quantifying individual camera-trap detection errors. The steps indicated are recommended to generate meaningful detection error terms that can be incorporated into further population-modelling exercises. [A]Animal movement speeds can likely either take the form of direct speed estimates from multiple camera -trap images in sequence (or video sequences), or alternatively from tracking/telemetry data if available for the study species. [B]Distances and angles from camera traps should ideally be marked out (e.g. Hofmeester *et al.* 2017), or at least estimated using measured distances to identifiable landmarks in the camera-trap field of view. [C]Many camera-trap models incorporate a built-in temperature sensor providing an estimate of the ambient temperature. While this may not always be reflective of overall ambient conditions, depending on camera trap placement (e.g. in direct sunlight vs in the shade), overall agreement with ambient temperatures seem reasonable (see Fig. S4).

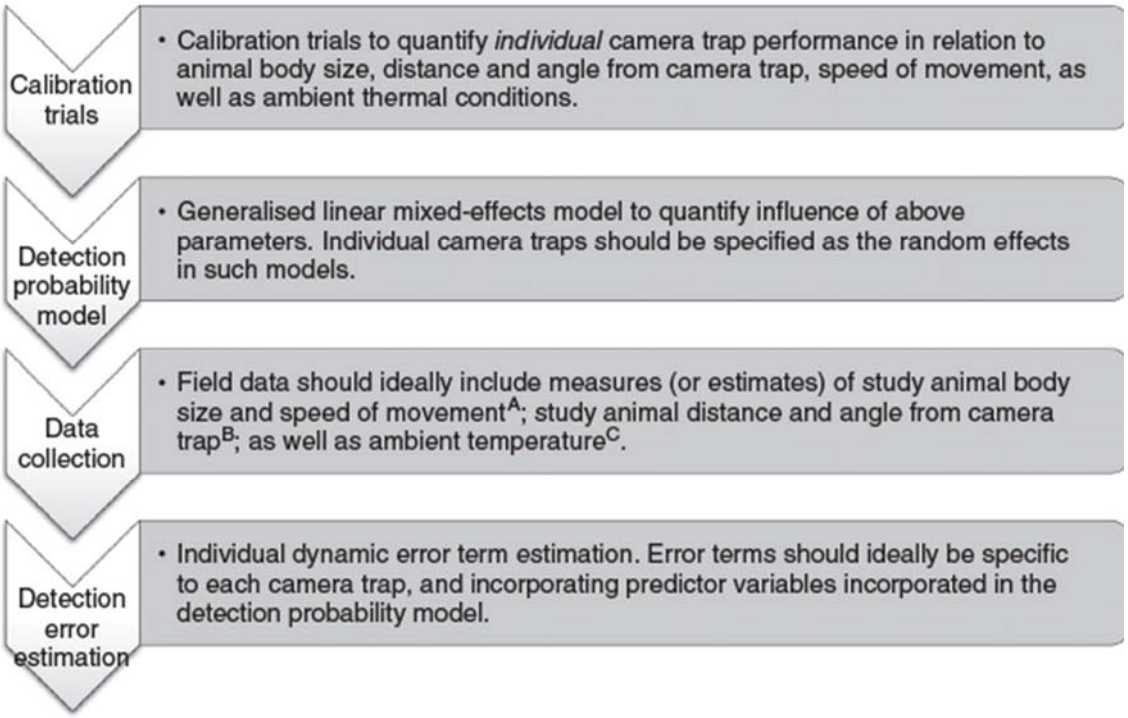

In summary, our results illustrated the influence of several factors on camera-trap detection probabilities inside camera-trap detection zones. Researchers should be aware of the limitations imposed by imperfect detections within the detection zones of camera traps, and

we recommend adequate individual camera-trap calibration and field measures to quantify likely effects on resulting research outcomes (Fig. 6).

Conflict of interest

The authors declare no conflicts of interest.

Acknowledgements

The following people are thanked for their assistance with running the camera trap/animal model trials: Arantxa Blecher, Andrea Webster, Marc Freeman, Johan van Wyk and Anabelle McIntyre. Two anonymous reviewers provided useful feedback on an earlier version of this paper. The Department of Science and Technology through the National Research Foundation of South Africa provided research funding support for the first author.

References

Anile, S., and Devillard, S. (2016). Study design and body mass influence RAIs from camera trap studies: evidence from the Felidae. *Animal Conservation* **19**, 35–45.

Apps, P., and McNutt, J. W. (2018). Are camera traps fit for purpose? A rigorous, reproducible and realistic test of camera trap performance. *African Journal of Ecology* **56**, 710–720.

Bates, D., Maechler, M., Bolker, B., and Walker, S. (2015). Fitting linear mixed-effects models using lme4. *Journal of Statistical Software* **67**, 1–48.
| Fitting linear mixed-effects models using lme4.Crossref | GoogleScholarGoogle Scholar |

Burton, A. C., Neilson, E., Moreira, D., Ladle, A., Steenweg, R., Fisher, J. T., Bayne, E., and Boutin, S. (2015). Wildlife camera trapping: a review and recommendations for linking surveys to ecological processes. *Journal of Applied Ecology* **52**, 675–685.

Calenge, C. (2006). The package adehabitat for the R software: a tool for the analysis of space and habitat use by animals. *Ecological Modelling* **197**, 516–519.

Caravaggi, A. (2017). remBoot: an R package for random encounter modelling. *The Journal of Open Source Software* **2**, 176.

Caravaggi, A., Zaccaroni, M., Riga, F., Schai-Braun, S. C., Dick, J. T. A., Montgomery, W. I., and Reid, N. (2016). An invasive-native mammalian species replacement process captured by camera trap survey random encounter models. *Remote Sensing in Ecology and Conservation* **2**, 45–58.

Cusack, J. J., Dickman, A. J., Rowcliffe, M. J., Carbone, C., Macdonald, D. W., and Coulson, T. (2015a). Random versus game trail-based camera trap placement strategy for monitoring terrestrial mammal communities. *PLoS One* **1**,

Cusack, J. J., Swanson, A., Coulson, T., Packer, C., Carbone, C., Dickman, A. J., Kosmala, M., Lintott, C., and Rowcliffe, J. M. (2015b). Applying a random encounter model to estimate lion density from camera traps in Serengeti National Park, Tanzania. *The Journal of Wildlife Management* **79**, 1014–1021.

Driessen, M. M., Jarman, P. J., Troy, S., and Callander, S. (2017). Animal detections vary among commonly used camera trap models. *Wildlife Research* **44**, 291–297.

Foster, R. J., Street, W., York, N., and Sciences, B. (2012). A critique of density estimation from camera-trap data. *The Journal of Wildlife Management* **76**, 224–236.

Hamel, S., Killengreen, S. T., Henden, J. A., Eide, N. E., Roed-Eriksen, L., Ims, R. A., and Yoccoz, N. G. (2013). Towards good practice guidance in using camera-traps in ecology: influence of sampling design on validity of ecological inferences. *Methods in Ecology and Evolution* **4**, 105–113.

Hijmans, R. J., Williams, E., and Vennes, C. (2017). geosphere: Spherical Trigonometry.

Hofmeester, T. R., Rowcliffe, J. M., and Jansen, P. A. (2017). A simple method for estimating the effective detection distance of camera traps. *Remote Sensing in Ecology and Conservation* **3**, 81–89.

Hofmeester, T. R., Cromsigt, J. P. G. M., Odden, J., Andren, H., Kindberg, J., and Linnell, J. D. C. (2019). Framing pictures: a conceptual framework to identify and correct for biases in detection probability of camera traps enabling multi-species comparison. *Ecology and Evolution* **9**, 2320–2336.

Howe, E. J., Buckland, S. T., Després-Einspenner, M. L., and Kühl, H. S. (2017). Distance sampling with camera traps. *Methods in Ecology and Evolution* **8**, 1558–1565.

Hughson, D. L., Darby, N. W., and Dungan, J. D. (2010). Comparison of motion-activated cameras for wildlife investigations. *California Fish and Game* **96**, 101–109.

Jacobs, C. E., and Ausband, D. E. (2018). An evaluation of camera trap performance: what are we missing and does deployment height matter? *Remote Sensing in Ecology and Conservation* **4**, 352–360.

Lewin-Koh, N. J., Bivand, R., Pebesma, E. J., Archer, E., Baddeley, A., Bibiko, H., Dray, S., Forrest, D., Friendly, M., Giraudoux, P., Golicher, D., Rubio, V., Hausmann, P., Hufthammer, K., Jagger, T., Luque, S., MacQueen, D., Niccolai, A., Short, T., Stabler, B., and Turner, R. (2011). 'maptools: Tools for Reading and Handling Spatial Objects. R Package Version 0.8-10.' Available at http://CRAN.R-project.org/package=maptools [verified 15 January 2019].

Lewis, J. S., Logan, K. A., Alldredge, M. W., Bailey, L. L., Vandewoude, S., and Crooks, K. R. (2015). The effects of urbanization on population density, occupancy, and detection probability of wild felids. *Ecological Applications* **25**, 1880–1895.

Lucas, T. C. D., Moorcroft, E. A., Freeman, R., Rowcliffe, J. M., and Jones, K. E. (2015). A generalised random encounter model for estimating animal density with remote sensor data. *Methods in Ecology and Evolution* **6**, 500–509.

Lüdecke, D. (2018). 'sjPlot: Data Visualization for Statistics in Social Science.' Available at https://zenodo.org/record/2400856#.XiAt9cgzZPY [verified 15 January 2019].

MacKenzie, D. I., Nichols, J. D., Lachman, G. B., Droege, S., Royle, J. A., and Langtimm, C. A. (2002). Estimating site occupancy rates when detection probabilities are less than one. *Ecology* **83**, 2248–2255.

Manzo, E., Bartolommei, P., Rowcliffe, J. M., and Cozzolino, R. (2012). Estimation of population density of European pine marten in central Italy using camera trapping. *Acta Theriologica* **57**, 165–172.

Marvin, D. C., Koh, L. P., Lynam, A. J., Wich, S., Davies, A. B., Krishnamurthy, R., Stokes, E., Starkey, R., and Asner, G. P. (2016). Integrating technologies for scalable ecology and conservation. *Global Ecology and Conservation* **7**, 262–275.

Meek, P. D., Ballard, G.-A., Fleming, P. J. S., Schaefer, M., Williams, W., and Falzon, G. (2014). Camera traps can be heard and seen by animals. *PLoS One* **9**, e110832.

Meek, P. D., Ballard, G.-A., and Fleming, P. J. S. (2015). The pitfalls of wildlife camera trapping as a survey tool in Australia. *Australian Mammalogy* **37**, 13–22.

Meek, P., Ballard, G., Fleming, P., and Falzon, G. (2016a). Are we getting the full picture? Animal responses to camera traps and implications for predator studies. *Ecology and Evolution* **6**, 3216–3225.

Meek, P. D., Ballard, G. A., and Falzon, G. (2016b). The higher you go the less you will know: placing camera traps high to avoid theft will affect detection. *Remote Sensing in Ecology and Conservation* **2**, 204–211.

Neilson, E. W., Avgar, T., Burton, A. C., Broadley, K., and Boutin, S. (2018). Animal movement affects interpretation of occupancy models from camera-trap surveys of unmarked animals. *Ecosphere* **9**, e02092.

Norouzzadeh, M. S., Nguyen, A., Kosmala, M., Swanson, A., Palmer, M. S., Packer, C., and Clune, J. (2018). Automatically identifying, counting, and describing wild animals in camera-trap images with deep learning. *Proceedings of the National Academy of Sciences of the United States of America* **115**, E5716–E5725.

O'Connell, A. F., and Bailey, L. L. (2011). Inference for occupancy and occupancy dynamics. In 'Camera Traps in Animal Ecology: Methods and Analyses'. (Eds A. F. O'Connell, J. D. Nichols, and K. U. Karanth.) pp. 191–205. (Springer: Tokyo, Japan.)

Pfeffer, S. E., Spitzer, R., Allen, A. M., Hofmeester, T. R., Ericsson, G., Widemo, F., Singh, N. J., and Cromsigt, J. P. G. M. (2018). Pictures or pellets? Comparing camera trapping and dung counts as methods for estimating population densities of ungulates. *Remote Sensing in Ecology and Conservation* **4**, 173–183.

R Core Team (2019). R: A language and environment for statistical computing. R Foundation for Statistical Computing, Vienna, Austria. Available at https://www.R-project.org/ [verified 17 January 2020.]

Randler, C., and Kalb, N. (2018). Distance and size matters: a comparison of six wildlife camera traps and their usefulness for wild birds. *Ecology and Evolution* **8**, 7151–7163.

Rowcliffe, J. M., Field, J., Turvey, S. T., and Carbone, C. (2008). Estimating animal density using camera traps without the need for individual recognition. *Journal of Applied Ecology* **45**, 1228–1236.

Rowcliffe, J. M., Carbone, C., Jansen, P. A., Kays, R., and Kranstauber, B. (2011). Quantifying the sensitivity of camera traps: an adapted distance sampling approach. *Methods in Ecology and Evolution* **2**, 464–476.

Stokeld, D., Frank, A. S., Hill, B., Choy, J. L., Mahney, T., Stevens, A., Young, S., Rangers, D., Rangers, W., and Gillespie, G. R. (2015). Multiple cameras required to reliably detect feral cats in northern Australian tropical savanna: an evaluation of sampling design when using camera traps. *Wildlife Research* **42**, 642–649.

Swann, D. E., Hass, C. C., Dalton, D. C., and Wolf, S. A. (2004). Infrared-triggered cameras for detecting wildlife: an evaluation and review. *Wildlife Society Bulletin* **32**, 357–365.

Tabak, M. A., Norouzzadeh, M. S., Wolfson, D. W., Sweeney, S. J., VerCauteren, K. C., Snow, N. P., Halseth, J. M., Di Salvo, P. A., Lewis, J. S., White, M. D., Teton, B., Beasley, J. C., Schlichting, P. E., Boughton, R. K., Wight, B., Newkirk, E. S., Ivan, J. S., Odell, E. A., Brook, R. K., Lukacs, P. M., Moeller, A. K., Mandeville, E. G., Clune, J., and Miller, R. S. (2018). Machine learning to classify animal species in camera trap images: applications in ecology. *Methods in Ecology and Evolution* **10**, 585–590.

Trolliet, F., Huynen, M., Vermeulen, C., and Hambuckers, A. (2014). Use of camera traps for wildlife studies. A review. *Biotechnologie, Agronomie, Société et Environnement* **18**, 446–454.

Welbourne, D. J., Claridge, A. W., Paull, D. J., and Lambert, A. (2016). How do passive infrared triggered camera traps operate and why does it matter? Breaking down common misconceptions. *Remote Sensing in Ecology and Conservation* **2**, 77–83.

Wickham, H. (2016). ‘ggplot2: Elegant Graphics for Data Analysis.’ (Springer-Verlag: New York, NY, USA.)